CO-Induced Modification of the Metal/MgO(100) Interaction

Henrik Grönbeck* and Peter Broqvist

Department of Applied Physics and Competence Centre for Catalysis, Chalmers University of Technology, SE-41296 Göteborg, Sweden

Received: July 11, 2003; In Final Form: September 4, 2003

CO-induced changes in the metal/metaloxide interaction of MgO(100)-supported palladium, silver, platinum, and gold in the form of atoms and layers have been investigated within the density functional theory. CO is found to modify the metal/MgO(100) interaction for atoms and one-atom-thick layers. Generally, the bond strength is enhanced, with the largest increase calculated for Pt (∼1 eV). For metal atoms, CO adsorption is found to increase the barrier of diffusion. The underlying mechanism for bond strengthening is traced back to a matching between the CO−metal and metal−metaloxide bond characteristics. The effect of support-induced changes for an arbitrary adsorbate−metal interaction is predicted to be small beyond three atomic layers.

I. Introduction

It is well established that adsorbates may have a pronounced effect on the stability of metal surfaces as well as structural properties of metal clusters. For example, the presence of CO is known to affect island shapes during homoepitaxial growth on Pt(111),[1] and ZnO-supported nanocrystals of copper have recently been found to undergo reversible structural changes as a response to the gaseous environment.[2] In ref 2, in situ transition electron microscopy measurements showed that an oxidizing atmosphere (hydrogen with water) resulted in spherical crystals, whereas a comparatively reducing atmosphere (hydrogen with CO) produced disklike structures. Similar observations have been reported for platinum islands grown on TiO_2,[3] where CO was found to induce wetting of the metal particles.

The fact that adsorbates can modify the structure of metal particles and thereby also induce changes in chemical characteristics has important implications for heterogeneous environmental catalysis where the active materials are known to be small particles of palladium, platinum, and rhodium dispersed on metal oxide supports. Another crucial issue within this field is to what extent adsorbates affect the metal/metaloxide interaction. Because sintering is the main reason for thermal deactivation of catalysts, it is important to understand the metal/metaloxide interaction and its response to adsorbates.[4] Currently, an overloading of expensive active material is needed to meet demands in durability. Adsorbate-induced effects of metal mobility were recently demonstrated for a platinum/$BaCO_3$ catalyst treated in O_2 and SO_2,[5] where the platinum particles were found to migrate several micrometers over the support in the presence of sulfur.

In the present paper, we have investigated issues related to adsorbate-induced modifications of the metal/support interaction by studying the interaction of adsorbates with two limits of supported metal: atoms and metal layers. As the metal oxide support we have chosen MgO(100). MgO(100) has become a standard model oxide surface for theoretical investigations.[6−9] The reason is twofold: MgO is comparatively easy to model and also routinely possible to prepare experimentally.[10] The investigated metals are palladium, platinum, silver, and gold. Palladium and platinum are currently used in automotive exhaust after-treatment catalysts. Small particles of gold have recently been demonstrated to have significant catalytic properties for CO oxidation.[11,12] Silver is included because structure and adsorption energetics of this metal have recently been studied by EXAFS[13] and calorimetry.[14] CO is chosen as an adsorbate because of the mentioned effects on the morphology of copper[2] and platinum[3] particles.

II. Computational Method

The computational approach is fairly standard:[15] the density functional theory (DFT)[16,17] in the plane wave and pseudopotential implementation. In particular, the Perdew−Burke−Ernzerhof (PBE) expression is used for the approximation of the exchange and correlation functional,[18] and ultrasoft scalar relativistic pseudopotentials are used to describe the interaction between the valence electrons and the core.[19,20] A kinetic cutoff energy of 28 Ry is used, yielding total energy convergence. The geometries were considered to be converged when the change in the total energy of the system was less than 1 meV, the root mean square of the forces was below 0.02 eV/Å, and the root mean square of the displacements was less than 0.001 Å.

Previous studies have shown that MgO(100) can be modeled with two atomic layers.[7,21] This is also done in the present work by keeping the bottom layer fixed at the theoretical lattice constant[22] while allowing the full structural relaxation of the top layer. In the modeling of adsorbed atoms, each layer contains 18 atoms (Figure 1). The metal films were modeled with the smallest possible cell: only one MgO unit per layer. The cell parameter perpendicular to the surface was 16 Å in the calculations of atoms and 22 Å in the calculation of the layers, ensuring convergence in the reported properties for all studied systems. *k* points were generated according to the Monkhorst−Pack scheme.[23,24] For the large surface model, two special *k* points were used, whereas the high-coverage limit utilized 25 special *k* points. Tests of the convergence with respect to the kinetic energy cutoff, *k*-point sampling, and cell sizes can be found elsewhere.[21,25]

* Corresponding author. E-mail: ghj@fy.chalmers.se.

10.1021/jp036004i CCC: $25.00
Published on Web 10/10/2003

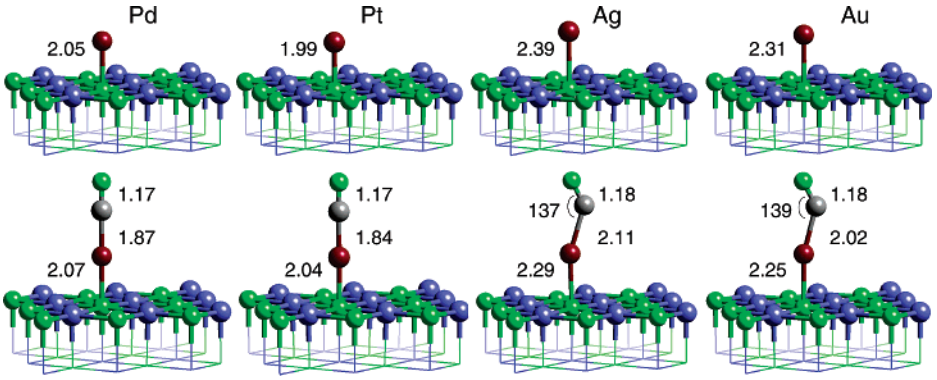

Figure 1. Structural models for adsorbed atoms and carbonyls. Top row from left to right: Pd, Pt, Ag, and Au. Bottom row: PdCO, PtCO, AgCO, and AuCO. The 4d and 5d metals are colored red (dark), Mg is blue (medium dark), and O is green (bright). Distances are in Å.

TABLE 1: Energetics of the Adsorbed Species

	Pd	PdCO	Pt	PtCO	Ag	AgCO	Au	AuCO
E_b[a]	1.52	1.76	1.54	2.48	0.47	0.68	0.92	0.89
ΔE_H[b]	0.46	0.75	0.93	1.10	0.13	0.26	0.25	0.37
ΔE_{Mg}[b]	1.00		2.04		0.27		0.49	

[a] Binding energy (eV) with respect to the gas-phase atoms. [b] ΔE_H and ΔE_{Mg} denote the energy differences (eV) between the stable oxygen site and the hollow and cation sites, respectively.

The gas-phase reference atoms and molecules were calculated in a periodic 12-Å box. The reference systems were calculated spin-polarized: CO, Pd, PdCO, and PtCO are singlets whereas Ag, AgCO, Au, and AuCO are doublets and Pt is a triplet. For the supported systems, only the lowest spin states were investigated; they are singlets in all cases except for Ag, AgCO, Au, and AuCO, which were calculated as doublets.

In other reports,[21,25] comparisons between the performance of the exchange correlation approximations used in the present study (PBE) and calculations using the local density approximation (LDA) have been made. The conclusions followed the general knowledge of these functionals. PBE reduces cohesion and predicts longer bond lengths in comparison with those predicted by LDA. In comparison to experiment, PBE is in overall better agreement, which has made us continue with this functional. However, it should be stressed that absolute binding energies are strongly dependent on the functional, and we should pay the most attention to relative stabilities and diffusion barriers.

III. Supported Atoms

With the choice of metals, we are studying 4d and 5d elements with 10 (Pd, Pt) and 11 (Ag, Au) valence electrons. Pd and Pt have different atomic ground states. Pd is $d^{10}s^0$, and Pt is d^9s^1. Although silver and gold have the same electronic ground state ($d^{10}s^1$), they are different with respect to d−s splitting. For the atoms, we calculate ∼2.7 eV for Ag and ∼0.8 eV for gold. Thus, a larger degree of s−d hybridization is expected for gold.

In Figure 1, the geometry-optimized structures for the studied systems are presented. Concentrating first on the bare metal atoms, we report in Table 1 the energetics for the three investigated sites: the anion site, the hollow site, and the cation site. For the anion site, the binding energy relative to the gas-phase metal atom is reported, whereas for the other two sites the relative stability with respect to the anion site is shown. For all four metals, atop the anionic oxygen represents the stable adsorption site. This is in agreement with previous studies of copper and nickel atoms.[7,26] In the stable configuration, a similar

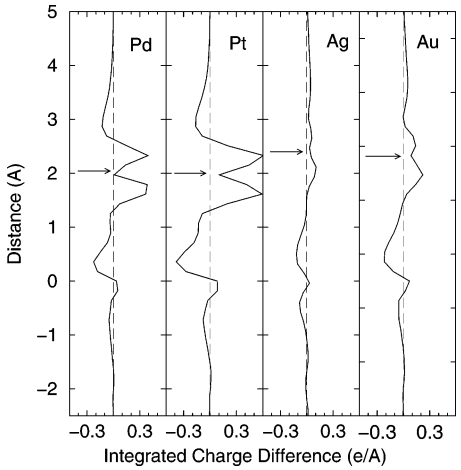

Figure 2. Integrated charge differences for supported Pd, Pt, Ag, and Au. The MgO(100) surface plane is located at zero distance. The locations of the metal atoms are indicated by arrows. The vertical dashed line is zero integrated charge difference.

absolute binding energy is calculated for Pd and Pt. The binding energy for Ag and Au is weaker, reflecting the closed d shell for these atoms. The large s−d splitting for Ag explains why this atom adsorbs with the lowest binding energy. The weaker bonds for the coinage metals are also reflected in longer (∼15%) bond lengths (Figure 1).

The differences in bonding of the metal atoms are clearly observed in an electronic charge difference analysis. The charge differences are calculated at the optimized geometries by (M denotes metal atom)

$$\delta\rho = \rho_{M/MgO} - \rho_M - \rho_{MgO}$$

Integrating $\delta\rho$ along the coordinate perpendicular to the surface yields a 2D measure of the charge rearrangement, shown in Figure 2 (the 3D $\delta\rho$ for Pt is shown in Figure 3). Upon Pd and Pt adsorption, metal states directed toward the surface (mainly d_{z^2}) polarize away from the surface to reduce the occupancy of antibonding combinations of metal d_{z^2} and oxygen p_z states. Moreover, the metal atoms gain stability by polarizing charge toward the surface cations. The charge redistribution is similar for Pd and Pt. Ag and Au clearly show less charge redistribution. The filled d shell reduces the possibility of charge polarization. If the charge difference is integrated along the surface normal, then a net charge transfer from the surface to the metal is obtained. The results from the integration are consistent with a Mulliken charge population analysis, yielding0.5, 0.45, 0.2, and 0.4 electrons for Pd, Pt, Ag, and Au, respectively.

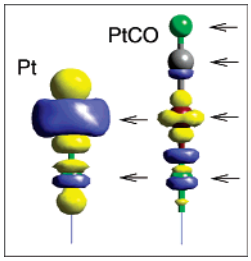

Figure 3. Charge differences for Pt and PtCO. Dark isosurface color indicates charge gain, whereas bright indicates charge depletion. Both isosurfaces are at an absolute value of 0.05 e/Å^3. Atomic positions are indicated by arrows. The color code is the same as that used in Figure 1.

On MgO(100), the hollow site represents the transition state between stable anionic sites. The barrier, ΔE_H, is reported in Table 1. A clear difference between the metals is predicted. Despite the similar stability for Pd and Pt at the atop site, the diffusion barrier is lower for Pd. The reason is most likely connected to the fact that the atomic configuration of the metal atoms at the hollow site contains less s contribution than at the atop site. Thus, the hollow site favors the atomic configuration of Pd. At the level of theory that we used, the Pt excitation energy from d^9s^1 to $d^{10}s^0$ is ∼0.5 eV, whereas the $d^{10}s^0$ to d^9s^1 excitation energy for Pd is ∼0.25 eV. Pd adsorbed on MgO-(100) has previously been investigated using PP−PW cluster calculations with an embedding potential.[9] E_b and ΔE_H were reported to be 1.16 and 0.43 eV, respectively, thus in good agreement with the present results. The calculated barriers for Ag and Au are lower than that for Cu, which previously has been calculated to be 0.45 eV using a scheme similar to ours.[7]

Following the work of ref 27, the activation temperature for diffusion (at least one jump between neighboring stable sites per second) using an Arrhenius expression can be estimated from the diffusion barrier. We find the activation temperature to be ∼180, 360, 50, and 100 K for Pd, Pt, Ag, and Au, respectively. Hence, the atomic diffusion of Pd, Ag, and Au would be possible to observe on experimental time scales at room temperature.

When introducing CO into the systems, we studied the case of adsorption on supported metal atoms. This is the only relevant site because the CO interaction with MgO(100) is weak.[28] Structural properties are shown in Figure 1. Binding energies together with relative stabilities at the hollow site are reported in Table 1. The MCO units are found to be more strongly bound to the surface than the corresponding bare atoms. The effect is most pronounced for PtCO, with an enhancement of ∼1 eV. To understand the striking difference in the adsorption of bare and CO-decorated metal atoms, the charge differences for Pt and PtCO were compared (Figure 3). For PtCO, the charge difference is calculated as $\delta\rho = \rho_{PtCO/MgO} - \rho_{PtCO} - \rho_{MgO}$. A clear difference is observed for the two cases. Whereas the charge redistribution for the bare atom includes only charge depletion in the Pt−O region, the PtCO/MgO(100) system shows charge accumulation in this bond. The d_{z^2} state of platinum, which for the bare atom is depopulated to form a net bonding with the surface, instead gains charge when PtCO adsorbs at the surface. The picture that emerges is that CO has prepared the Pt atom for bonding to the oxygen anion. The M−CO bond is commonly understood in the 5σ donation and 2π* back-donation model.[29] This implies that the CO 5σ state has polarized Pt in a way that is similar to the surface anion polarization of the bare metal atom. The same reasoning applied to the M−CO bond suggests that CO should be more strongly bound to the adsorbed metal atom than to the corresponding gas-phase atom. This is also what is calculated. In the gas phase, the PdCO and PtCO bond strengths are 2.45 and 2.70 eV, respectively, whereas the corresponding values on the adsorbed metal atoms are 2.69 and 3.63 eV. In the case of supported AgCO and AuCO, small changes with respect to the bare metal atom are observed, 0.21 and −0.03 eV, respectively. For silver, the difference can be attributed to the rehybridization caused by the adsorbate. The gas-phase Ag−CO and Au−CO binding energies are calculated to be 0.41 and 0.96 eV, respectively. Thus, the bond is merely of the polarization type. One indication of this type of bond is the low integrated electronic charge distribution along the M−CO bond. At half of the bond distance, this value is 1.2 and 1.7 e/A for Ag and Au, respectively. The corresponding values for the transition-metal atoms are 2.1 (Pd) and 2.5 (Pt) e/A.

For PdCO and PtCO, the metal−surface bond is longer than for the bare metal atom (Figure 1). This is rationalized by the change in bond characteristics discussed above. CO adsorption induces more covalent metal−anion bond character, with charge accumulation between the metal and surface. For Ag and Au, the filled d shell results in a different trend yielding a shorter M−surface bond for MCO. CO slightly rehybridizes the noble-metal atoms but does not change the character of the bond as in the cases of Pd and Pt.

A striking difference is observed between the transition metals and the noble metals in the M−CO configuration. AgCO and AuCO are not linear but instead have an angle of ∼140°. The bent structure arises so as to minimize Coulomb repulsion and kinetic energy in the (Ag−C and Au−C) antibonding singly occupied HOMO (highest occupied molecular orbital). This orbital can be characterized as an antibonding combination of CO(5σ) and a 6s−5d_{z^2} hybrid. The angle is virtually unchanged when going from the gas phase to the adsorbed units. Using a computation method similar to the present one, Häkkinen and Landman recently reported an angle of 132° for CO adsorption in the top configuration at anionic Au_2^-.[30]

Comparing the relative stability of the atop and hollow configurations, it is found that the barrier for anion-to-anion diffusion is *increased* upon CO adsorption. This observation is understood by the increased stability of the atop site thanks to bond matching. The effect is ∼0.2 for Pd and Pt and ∼0.1 for Ag and Au. Experimentally, CO oxidation over MgO-supported Pd atoms has been investigated using mass spectrometry and infrared spectroscopy.[9] On the basis of changes in the CO stretching vibration, it was suggested that PdCO units could migrate over MgO(100) terraces at temperatures below room temperature. The calculated barrier (0.75 eV) is low enough for such diffusion to be possible.

IV. Supported Layers

Atomic adsorption is a limiting case with no metal−metal interaction. To investigate how the metal/metal oxide interface respond to CO adsorption in the presence of metal−metal bonds, the other limit has also been studied, namely, layers of metal atoms. To this end, metal layers with the first layer occupying oxygen anion sites have been explored. We call these types of layers equioxygen atomic layers (EOALs).[21] The studied layers correspond to 0.71, 0.75, 0.80, and 0.81 of a monolayer with (111) packing for Pd, Pt, Ag, and Au, respectively.[31] The calculations are made with the smallest possible unit cell that reduces the possibility of structural relaxation. However, the metal/metal oxide lattice mismatches are small (0.91, 0.93, 0.96, and 0.97 for Pd, Pt, Ag, and Au, respectively), and explicit

TABLE 2: Energetics and Selected Bond Distances for Metal EOALs on MgO(100)[a]

	E_b^{M}[b]	E_b^{MCO}[b]	d_{O-M}^{M}[c]	d_{O-M}^{MCO}[c]
Pd(1)	0.70	1.17	2.23	2.16
Pd(2)	0.48	0.54	2.33	2.33
Pt(1)	0.57	1.42	2.30	2.16
Pt(2)	0.47	0.50	2.37	2.36
Ag(1)	0.16		2.75	
Ag(2)	0.27	0.34	2.61	2.46
Au(1)	0.13		2.87	
Au(2)	0.30	0.29	2.60	2.64

[a] (1) and (2) indicate the number of metal layers. [b] E_b^{M} and E_b^{MCO} (eV) denote the binding of bare and CO covered EOALs to the support, respectively. [c] d_{O-M}^{M} and d_{O-M}^{MCO} (Å) are the corresponding metal to surface oxygen bond distances.

calculations for Pt in a double-sized cell have verified the validity of this approach.[21] Moreover, EXAFS measurements for Ag/Mg(100) have suggested (100) metal growth with Ag atoms bonded to surface anions.[13] CO adsorption on the EOALs is studied in the atop configuration. The explored systems correspond to a high coverage with considerable repulsive direct and surface-mediated CO−CO interaction. The direct repulsion is estimated by calculating a CO array without metal and support to 0.15 eV per CO unit.

The results for the bare and CO-decorated EOALs are collected in Table 2. We note that the binding energies of the bare metal films to the support are weak. This has previously been reported for various transition-metal films adsorbed on Al_2O_3.[32] For EOALs of Pd and Pt, the addition of a second layer (over the cation site) reduces the binding energy slightly. For Ag and Au, the reversed situation applies, owing to the induced metal rehybridization. A low adhesion of silver particles to MgO(100) has been measured using calorimetry.[14] In ref 14, the Ag−MgO(100) bond energy for large 3D particles was determined to be 0.16 ± 0.16 eV. However, the good agreement between experimental data and the present calculations may be accidental. The metal−MgO(100) bond is a polarization bond, and it has recently been pointed out that gradient-corrected density functionals (such as the one applied in the present work) may predict bond strengths of such bonds in some error because of electron self-exchange and self-correlation.[33] Therefore, it should be stressed that trends in Table 2 are more relevant than absolute binding energies.

The poor binding of the EOALs to the support is also manifested in the long M−O bond distances, which are ∼15% longer than for the single metal atoms. The surface Ag−O bond length of thin Ag films grown on MgO(100) has been estimated experimentally from EXAFS measurements to be 2.53 ± 0.05 Å.[13] Thus, the structural data for Ag are in fair agreement with experiment.

Adsorbing CO on one layer of Pd and Pt has a significant effect on the metal/MgO(100) binding energy. Per atom, the effect is of the same order of magnitude as that for the single atoms. Because of the high coverage, CO adsorption on M(1) is not stable for silver and gold. The strong metal−MgO(100) bond enhancement owing to the CO molecule for palladium and platinum vanishes for two metal layers. For these systems, the binding energies are similar to those of the bare counterparts. This is not surprising because the mechanism for bond stabilization in the case of single-layer EOAL is the metal-bond preparation induced by CO.

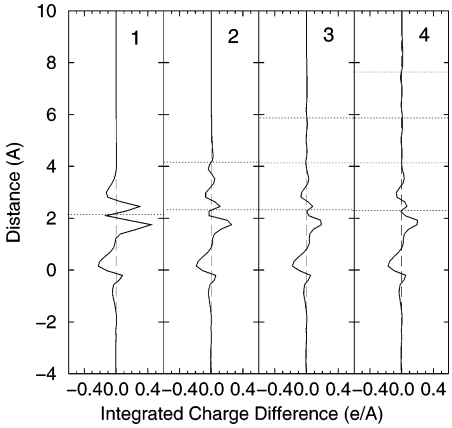

Figure 4. Integrated charge differences for one to four EOALs of platinum adsorbed onto MgO(100). The MgO(100) surface plane is located at zero distance. The metal planes are indicated by dotted lines. The vertical dashed line is zero integrated charge difference.

Because CO has been observed to have a wetting effect on TiO_2-supported platinum particles,[3] it is interesting to analyze the relative stability of layered systems with respect to the total cohesion of platinum. The cohesion of the metal has three contributions: metal/metal, metal/metal oxide, and CO−metal. Among these, the metal−metal interaction is the strongest. The bulk metal cohesion is calculated to be 4.7 eV for Pt.[31] The CO−Pt(100)/MgO(100) bond is calculated to be 2.50 and 1.59 eV for the supported one- and two-layer systems, respectively.[34] Thus, for one metal layer, bond preparation results in a significant bond strengthening.[35] For the bare layers, the average cohesion increases from 2.56 to 3.63 eV when going from the single to the double layer. Calculating the total average cohesion for the CO-covered layers, we find that Pt in CO−Pt(1) has higher cohesion than Pt in CO−Pt(2), 5.03 eV compared with 4.43 eV. This is not what the simple addition of bond strengths would suggest. Because CO is bonded by ∼1.6 eV to an unsupported metal system and the metal−metal cohesion is large, such arguments would instead favor the CO−Pt(2) configuration. However, the bond-preparation mechanism energetically drives the Pt/MgO(100) system to the single-layer configuration. In ref 3, it was argued that the observed wetting could be a result of the stabilization by CO adsorption on an increased number of platinum surface sites. The present calculations propose an additional mechanism that energetically would work in the same direction.

A general issue is how many metal layers are needed for an arbitrary adsorbate and the metal support to decouple. Knowing that the screening length in metals is about 1 nm, the effects of metal/adsorbate interactions should not extend to more than roughly three metal overlayers. In an effective medium picture, adsorbates and the support decouple if the change in the electronic density of the metal due to the support at the topmost layer is small. To illustrate this, we report in Figure 4 the charge difference for one to four Pt EOALs on MgO(100). The effect of the support on one layer is strong (left panel). The charge depletion that facilitates the CO adsorption is clearly observed. For two layers, the effect of the support on the topmost density is smaller, and for three and four layers, the deviation from the bare metal system is small. Thus, from these calculations the effect of support-induced changes in the adsorbate−metal interaction is predicted to be small beyond three atomic layers.

V. Conclusions

We have performed first principles calculations to investigate adsorption on metal/metal oxide systems. In particular, we have studied the effect of the support on the adsorbate/metal bond and the effect of the adsorbates on the metal/metal oxide interface. For atoms of Pd, Pt, and Ag, we find that CO enhances the M/MgO(100) interaction and increase diffusion barriers. The reason for the higher diffusion barriers is mainly the stabilization of the atop oxygen configuration owing to similarities in the M−O and CO−M bonds. The results indicate that the presence of CO would slow sintering caused by atomic diffusion (i.e., Ostwald ripening).

By studying EOALs of the different metals, it was possible to show that CO-induced bond stabilization is also present for single EOALs of palladium and platinum. This observation could be important in view of the wetting of platinum particles on TiO_2 observed in the presence of CO.[3] In this context, however, it is important to investigate the effect of CO on platinum self-diffusion.

Note Added in Proof. After the submission of this work, two papers have appeared on the interaction between CO and MgO-supported atoms of Rh, Pd, and Ag.[36,37] These publications agree on one of the main findings in the present work, namely, that PdCO is more strongly bonded to a MgO(100) terrace than Pd is.

Acknowledgment. Some of the calculations were performed at the Center for Parallel Computing, Sweden. We thank Itai Panas, Magnus Skoglundh, and Bengt Kasemo for valuable discussions. This work was performed at the Competence Centre for Catalysis hosted by Chalmers University of Technology and was financially supported by the Swedish Energy Agency and member companies AB Volvo, SAAB Automobile Powertrain AB, Johnson Matthey CDS, Perstorp AB, Akzo Nobel, MTC AB, and the Swedish Space Corporation.

References and Notes

(1) Kalff, M.; Comsa, G.; Michely, T. *Phys. Rev. Lett.* **1998**, *81*, 1255.
(2) Hansen, P. L.; Wagner, J. B.; Helveg, S.; Rostrup-Nielsen, J. R.; Clausen, B. S.; Topsøe, H. *Science* **2002**, *295*, 2053.
(3) Steinrück, H.-P.; Pesty, F.; Zhang, L.; Madey, T. E. *Phys. Rev. B* **1995**, *51*, 2427.
(4) Bartholomew, C. H. *Appl. Catal., A* **2001**, *212*, 17.
(5) Grant, A. W.; Amberntsson, A.; Fridell, E., to be published, 2003.
(6) Yudanov, I.; Pacchioni, G.; Neyman, K.; Rösch, N. *J. Phys. Chem. B* **1997**, *101*, 2786.
(7) Musolino, V.; Selloni, A.; Car, R. *J. Chem. Phys.* **1998**, *108*, 5044.
(8) Musolino, V.; Selloni, A.; Car, R. *Phys. Rev. Lett.* **1999**, *83*, 3242.
(9) Abbet, S.; Heiz, U.; Häkkinen, H.; Landman, U. *Phys. Rev Lett.* **2001**, *86*, 5950.
(10) Campbell, C. T. *Surf. Sci. Rep.* **1997**, *27*, 1.
(11) Sanchez, A.; Abbet, S.; Heiz, U.; Häkkinen, H.; Barnett, R. N.; Landman, U. *J. Phys. Chem. A* **1999**, *103*, 9573.
(12) Molina, L. M.; Hammer, B. *Phys. Rev. Lett.* **2003**, *90*, 206102.
(13) Flank, A. M.; Deaunay, R.; Lagarde, P.; Pompa, M.; Jupille, J. *Phys. Rev. B* **1996**, *53*, R1737.
(14) Larsen, J. H.; Ranney, J. T.; Starr, D. E.; Mugrove, J. E.; Campblell, C. T. *Phys. Rev. B* **2001**, *63*, 195410−195411.
(15) Payne, M. C.; Teter, M. P.; Allan, D. C.; Arias, T. A.; Joannopoulos, J. D. *Rev. Mod. Phys.* **1992**, *64*, 1045.
(16) Hohenberg, P.; Kohn, W. *Phys. Rev.* **1964**, *136*, 864.
(17) Kohn, W.; Sham, L. J. *Phys. Rev.* **1965**, *140*, A1133.
(18) Perdew, J. P.; Burke, K.; Ernzerhof, M. *Phys. Rev. Lett.* **1996**, *77*, 3865.
(19) Vanderbilt, D. *Phys. Rev. B* **1990**, *41*, 7892.
(20) The ultrasoft potentials distributed together with the CASTEP code from Accelrys were used. For the different atoms, the number of electrons treated in the valence are C(4), O(6), Mg(8), Pd(10), Pt(10), Ag(11), and Au(11). The applied pseudopotentials were generated with the same approximation to the exchange and correlation functional (PBE) as was used in the calculation.
(21) Grönbeck, H.; Broqvist, P. *J. Chem. Phys.* **2003**, *119*, 3896.
(22) The lattice constant, cohesion, and bulk modulus for MgO were calculated to 4.30 Å, 9.6 eV, and 1.4 Mbar. The experimental values are 4.21 Å,[38] 10.4 eV, and 1.5 Mbar,[39] respectively.
(23) Monkhorst, H. J.; Pack, J. D. *Phys. Rev. B* **1976**, *13*, 5188.
(24) Pack, J. D.; Monkhorst, H. J. *Phys. Rev. B* **1977**, *16*, 1748.
(25) Broqvist, P.; Grönbeck, H.; Panas, I., to be submitted for publication.
(26) Pacchioni, G.; Rösch, N. *J. Chem. Phys.* **1996**, *104*, 7329.
(27) Stumpf, R.; Scheffler, M. *Phys. Rev. Lett.* **1994**, *72*, 254.
(28) Illas, F.; Pacchioni, G.; Pelmenschikov, A.; Pettersson, L. G. M.; Dovesi, R.; Pisant, C.; Neyman, K. M.; Rösch, N. *Chem. Phys. Lett.* **1999**, *306*, 202.
(29) Blyholder, G. *J. Phys. Chem.* **1964**, *68*, 2772.
(30) Häkkinen, H.; Landman, U. *J. Am. Chem. Soc.* **2001**, *123*, 9704.
(31) The lattice constants and cohesion for the bare metals were calculated to be 3.92 Å and 3.8 eV (Pd), 4.00 Å and 4.7 eV (Pt), 4.14 Å and 2.6 eV (Ag), and 4.18 Å and 3.1 eV (Au). The corresponding experimental data (*American Institute of Physics Handbook*; Gray, D. E., Ed.; McGraw-Hill: New York, 1972) are 3.89 Å and 3.9 eV (Pd), 3.92 Å and 5.8 eV (Pt), 4.08 Å and 2.8 eV (Ag), and 4.07 Å and 3.8 eV (Au). In the calculation of the bulk properties, 35 special *k* points were used.
(32) Bogicevic, A.; Jennison, D. R. *Phys. Rev. Lett.* **1999**, *82*, 4050.
(33) Mattson, A. E.; Jennison, D. R. *Surf. Sci.* **2002**, *520*, L611.
(34) The corresponding binding energies (eV) for the other systems are 1.82 (CO−Pd(1)), 1.17 (CO−Pd(2)), 0.35 (CO−Ag(2)), and 0.41 (CO−Au(2)).
(35) The CO−metal bond strength for the present systems may be compared with 1.53 eV for atop adsorption on Pt(111), which has been calculated within the same computational scheme as the present.[21]
(36) Judai, K.; Abbet, S.; Wörz, A.; Heiz, U.; Giordano, L.; Pacchioni, G. *J. Phys. Chem. B* **2003**, *107*, 9377.
(37) Giordano, L.; Vitto, A. D.; Pacchioni, G.; Ferrari, A. M. *Surf. Sci.* **2003**, *540*, 63.
(38) *CRC Handbook of Chemistry and Physics*; Lide, D. R., Ed.; CRC Press: Boca Raton, FL, 1999.
(39) Chang, Z. P.; Barsch, G. R. *J. Geophys. Res.* **1969**, *74*, 3291.